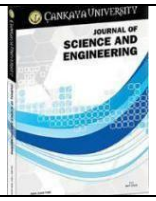
**e-ISSN:** 2564-7954 CUSJE 23(1): 033-045 (2026) Research Article



Çankaya University

**Journal of Science and Engineering**

https://dergipark.org.tr/cankujse

CUJSE

# Implementation of an Optical Tactile Sensing System with Machine Learning

Yusuf Buğra Günaydın[1*], Elif Safel[1], Ahmet Gökay Çalış[1],Çağlar Arpali[1]

[1] Department of Mechatronics Engineering, Çankaya University, Eskişehir Yolu 29.Km, 06790 , Ankara/TÜRKİYE

**Keywords**

Artificial Neural Networks,
Machine Learning,
Optical Tactile Sensors,
Pattern Recognition,
Tactile Sensors.

**Abstract**

In this study, a cost-effective tactile sensing system based on optical sensing technology was developed. The proposed system consists of a 4×4 sensor array designed for surface shape detection and force-based signal acquisition under external loading. During operation, the applied force is converted into an optical signal, and the acquired sensor outputs are classified by an artificial neural network (ANN) model. Variations in surface patterns, such as flat, wavy, and edged structures, produce different optical intensity distributions depending on the applied force, enabling the recognition of surface characteristics. Using only 16 sensors, the developed system achieved effective surface classification with a spatial force sensitivity of 2.15 N/cm². The ANN-based model achieved a surface profile identification accuracy of 94.2%. The developed sensing system offers a low-cost and effective solution for applications requiring surface recognition and object classification in automotive, industrial and robotic systems.

## 1.Introduction

As a result of the development of technology and the efforts to significantly reduce human needs, industrial robots are increasingly taking over tasks. The capabilities of industrial robots, which are of great importance, especially in areas requiring micro-processing such as production, biomedical, and healthcare, vary [1]. As these robots continue to develop, they are expected not only to perform their intended tasks but also to adapt to changing environments, support autonomous operation, and enable safe interaction [2]. In this context, tactile sensing plays an important role by allowing robotic systems to perceive and interpret physical contact. Tactile sensors required for this interaction are often costly, since high resolution, sensitivity, and reliability are generally expected at the same time during operation [3].

Inspired by the human sense of touch, tactile sensing systems have been developed to detect and interpret mechanical stimuli generated during contact. In humans, touch perception is generally modeled through cutaneous and kinesthetic sensing. Cutaneous sensing is associated with stimuli acting on the skin surface, while kinesthetic sensing is related to receptors in muscles, tendons, and joints [4]. In robotic applications, tactile sensors serve as the interface that captures such contact-related information and converts it into measurable electrical or optical signals [3], [4]. Tactile sensing has therefore become an essential perception modality in robotic manipulation, especially in applications where force distribution, surface condition, slip, or local contact geometry cannot be estimated reliably through remote sensing alone. In addition to robot hands and grippers, tactile sensing has also been studied in automation, biomedical instrumentation, human–robot interaction, and minimally invasive procedures [1]–[3].

* Corresponding Author: gunaydin911@gmail.com
Received: March 25, 2025, Accepted: April 7, 2026

A wide range of tactile sensing principles has been explored in the literature, including piezoresistive, capacitive, piezoelectric, inductive, triboelectric, and optical approaches [2], [3]. These sensing mechanisms differ in terms of sensitivity, repeatability, fabrication complexity, robustness, hysteresis, and susceptibility to electromagnetic interference. As a result, no single tactile sensing principle can simultaneously maximize sensitivity, manufacturability, robustness, and low cost for every robotic application [2]–[4]. In practice, high sensitivity, sufficient spatial resolution, robustness, and repeatability are often expected simultaneously, which makes tactile sensing system design challenging and, in many cases, costly [2], [3].

Among the available approaches, optical tactile sensing has attracted particular attention because of its wide sensing area, reusability, and immunity to electromagnetic interference [3], [5], [6]. Optical tactile sensors generally employ a deformable contact surface, a light source, and an imaging or light-detection mechanism to interpret surface deformation and contact behavior. Such systems are often capable of providing dense tactile information and high spatial resolution while being immune to electromagnetic interference [3], [5], [6]. However, many optical tactile sensing systems rely on relatively complex and expensive hardware, such as cameras, fiber-optic elements, and demanding calibration or alignment procedures [5]–[7]. Although these methods can provide high-quality tactile information, their hardware burden may limit their use in practical low-cost robotic applications.

One of the most influential examples in the field is GelSight, which demonstrated that a soft optical tactile sensor can estimate contact geometry and force-related information through detailed observation of elastomer deformation [7]. This work had a strong impact on later optical tactile sensing studies by showing that high-resolution visual deformation analysis can provide rich tactile perception. Similarly, TacTip introduced a family of soft optical tactile sensors inspired by the morphology of the human fingertip and showed that compliant, biomimetic tactile sensing structures can be adapted to different robotic applications [8]. Another important step in the literature was the development of more compact and accessible optical tactile sensors. DIGIT was introduced as a low-cost, compact, and high-resolution tactile sensor suitable for in-hand manipulation tasks, helping optical tactile sensing move closer to practical robotic deployment [9]. More recently, Evetac extended this concept by using an event-based camera instead of a conventional RGB camera, enabling higher temporal responsiveness and improved performance in dynamic tactile events such as slip and vibration [10]. These studies show that optical tactile sensing continues to evolve not only in sensing quality but also in compactness and temporal capability.

In addition to camera-centered optical systems, several studies have explored fiber-based tactile sensing architectures. Sato et al. developed a finger-shaped GelForce sensor capable of measuring surface traction fields for robotic hands, demonstrating that optical tactile sensing can be implemented in finger-like structures suitable for dexterous interaction [11]. Xie et al. proposed a pixel-based optical fiber tactile force sensor for robot manipulation, in which force-related information was estimated through changes in light intensity [12]. Kampmann and Kirchner presented a multi-modal tactile sensing system for underwater manipulation that combined fiber-optic and piezoelectric sensing principles, illustrating the adaptation of tactile sensing to harsh and visually challenging environments [13]. Another branch of the literature has focused on embedding optical or fiber-based tactile sensing into robotic skins and manipulators. Massari et al. integrated Fiber Bragg Grating strain sensors into a tactile sensing structure for a robotic manipulator and showed that tactile feedback can improve both control and object interaction performance [14]. Kappassov et al. also proposed a color-coded fiber-optic tactile sensor for an elastomeric robot skin, where optical fibers and a color camera were used to estimate contact-related information on a deformable surface [15]. These studies suggest that distributed tactile sensing over soft surfaces remains an active and promising area in robotic interaction research.

Beyond industrial robotics, tactile sensing concepts have also been investigated in biomedical applications. Jeong et al. reported a triboelectric touch sensor for position mapping during total hip arthroplasty, showing that tactile sensing principles can be used in medical tools and contact-aware clinical procedures [16]. This broader perspective indicates that tactile sensing is important not only for robotic manipulation but also for healthcare, monitoring, and contact-sensitive human-centered systems.

Overall, the literature reveals a clear trade-off. High-performance optical tactile systems are often based on cameras, fiber-optic structures, or complex illumination and calibration setups, which improve sensing quality but also increase cost, system size, alignment difficulty, and computational load [5]–[15]. Therefore, despite the advantages of optical tactile sensing, there remains a clear need for simpler, lower-cost, and easier-to-integrate optical tactile sensor designs for practical robotic use.

In this context, the present study proposes an LED-based optical tactile sensing approach that reduces hardware complexity while still providing effective pattern classification performance. The developed system uses a 4×4 sensor array consisting of 16 sensors and detects deformation caused by physical contact without camera-based imaging. The acquired sensor signals are processed using an artificial neural network (ANN)-based classification approach for the recognition of different surface patterns. The system was evaluated using five different surface classes, and the proposed ANN-based model achieved a classification accuracy of 94.2%. In addition to its classification performance, the system maintains a low total cost of approximately 20 USD, making it a practical and economical alternative for applications requiring surface recognition and object classification in automotive, industrial, and robotic systems. In this respect, the study contributes both to the development of simplified optical tactile sensing hardware and to the effective use of machine learning-based classification in low-cost tactile sensing applications.

## 2.Methods

This study aims to design and implement an optical tactile sensing system to recognize and classify the shape of objects. The system was designed to distinguish variations in the surface patterns of objects and categorize these shapes into distinct groups. The basic component of the system is based on the optical-based force sensor produced by us. After ensuring its accuracy, a sensor array consisting of 16 sensors was created and integrated into the custom-designed gripper. Upon completion of the system implementation, a series of tests was conducted to evaluate the system's ability to categorize different surface shapes accurately and reliably. After the theoretical studies of designing the optical tactile sensing system were completed, calibration operations were carried out. To calibrate the sensors, the same weights were tested with a well-known force sensor, the RP-S40-ST, known to comply with golden standards. This led to a comparative analysis between the two systems. Following the successful calibration phase, the system was integrated into the custom-designed robot arm, enabling it to grasp objects with various surface properties. Subsequently, the data collected from the sensors underwent training and testing using MATLAB-based artificial neural networks. This comprehensive study includes the following parts: Mechanical design, sensor design, and software design, all contributing to the creation of a robust and reliable tactile sensing system.

### 2.1. Mechanical Design

The mechanical structure of the system was designed to provide controlled gripping motion and stable contact between the object surface and the sensor array. The proposed mechanism consists of a bottom fixed sensor platform and an upper moving gripper structure. The upper part is responsible for applying force to the target object so that the surface pattern can be transferred to the sensors in a repeatable manner. The mechanical components were first modeled in CAD and then fabricated using a 3D printer. The overall structure was designed to ensure proper alignment between the moving gripper and the sensing region. A rack-and-pinion-based transmission mechanism was used to convert the rotational motion of the motor into linear motion. The gear design can be expressed with the following formula $m = d/N$ where $m$ represents the ratio between the pitch diameter and the number of teeth, $N$ represents the number of teeth, and $d$ is the pitch diameter in mm [13]. For $\text{Gear}_1$, the ratio was set to 1.5 $m_1 = 56/36$, and $\text{Gear}_2$ ratio was set to 1.66 $m_2 = 40/24$ so that it could hold objects without damaging them. A brushless DC electric motor, NEMA 23 with a step angle of 1.8 degrees, was used for mobility and compression in the mechanical design, thus providing a linear spatial resolution of 1.12 mm along y axis. This ensured gentle holding. This configuration allowed the upper gripper to move vertically and apply force to the object placed on the sensor array. The actuation system was designed to provide sufficient

holding force while maintaining controlled displacement. The motor drives the transmission mechanism and enables the gripper to move downward until contact is established with the object surface. The applied force allows the surface geometry of the object to be reflected on the sensor outputs through the deformation of the sensing structure. The designed robotic system weighs approximately 4 kg post-assembly and wiring, shown in Figure 1. Thus, designed system ensures standardized and repeatable loading conditions during the data collection process.

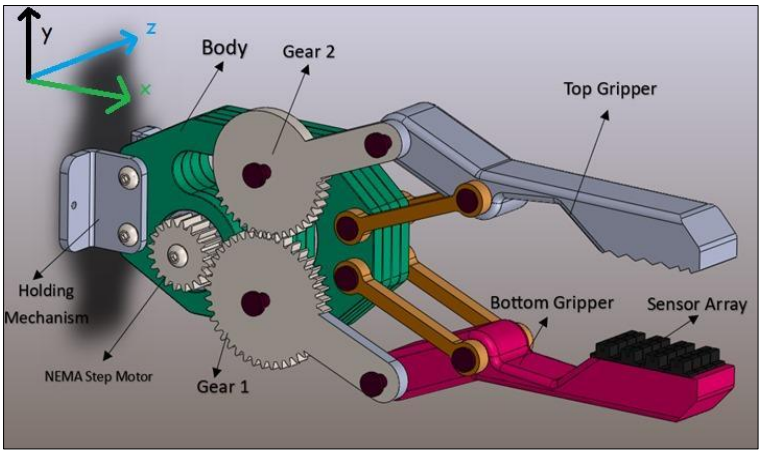



**Figure 1.** Gripper system

## 2.2.Electronic Design

### 2.2.1.Sensor Design

In this study, a sensor consisting of a gallium arsenide infrared emitting diode and a silicon phototransistor housed in a plastic package was used with a spacing of 7 mm. For each sensor, a blocker mechanism was designed to interrupt the light path between the emitting diode and the phototransistor. This mechanism was designed in CAD and fabricated using PLA material with a 3D printer. The system also includes two springs for each sensor.

The purpose of this mechanism is to allow linear downward motion under an applied load and to insert the blocker part between the emitting diode and the phototransistor. As a result, the sensor voltage decreases and the output value approaches zero. In this way, the presence of a load on the sensor can be detected. For example, when the object gripped by the gripper has a flat surface, most or a certain group of sensors produce consecutive values close to zero. In contrast, when the object has an irregular serrated surface, non-consecutive and more distant sensors tend to produce values close to zero.

An experiment was conducted to find out the spring constant $F=k\Delta x$ of the springs used in this system, where F is the applied force, k is the spring constant, and Δx is the amount of compression, since it was not known. The amount of compression of the spring was measured by increasing the force applied to a single spring in the experiment. The curve fitting method was used to reach the experimental result with the data that was received. Using the spring constant formula of the experimental data, the spring constant was calculated, which is k = 0.098 N/mm.

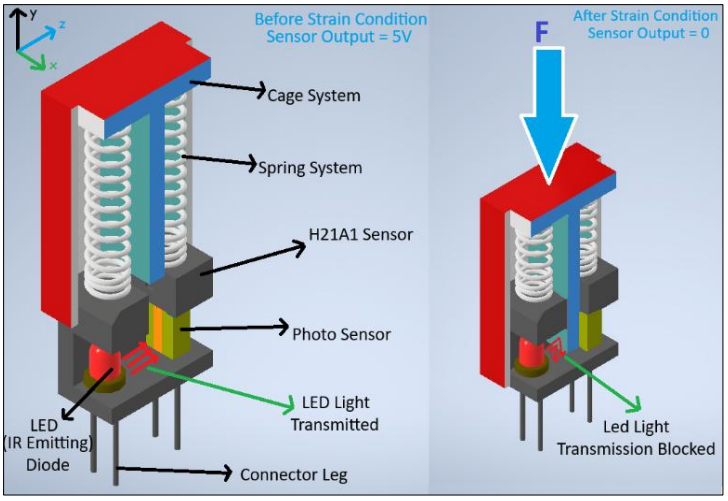



**Figure 2.** Designed sensor

### 2.2.2.Sensor Comparison

In the market research, the RP-S40-ST force sensor was selected for comparison with the designed sensor. The graph was drawn after the normalization according to the maximum value obtained by different forces applied on the sensor. The mV produced voltage with respect to force is given below.

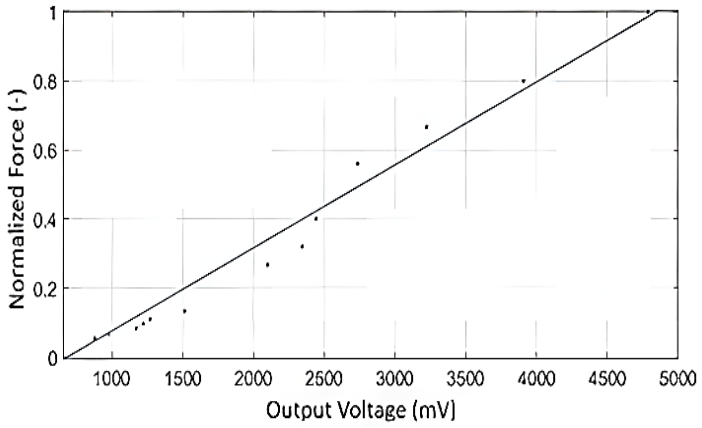



**Figure 3**. Reference force sensor (RP-S40-ST): Normalized Force vs Output Voltage (mV)

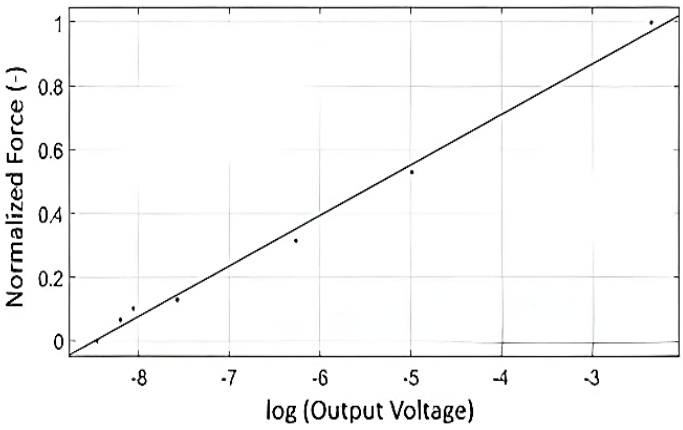



**Figure 4.** Proposed optical sensor (linearized): Normalized Force vs log (Output Voltage)

The change in the $mV$ value measured by the sensor as the force on the sensor increases is shown in Figure 3 and 4. These two graphs illustrate the different behaviors of the sensors. Figure 3 shows the linear force-stress relationship of the commercial reference force sensor. In contrast, Figure 4 shows the linearized form of the raw data of the proposed optical sensor, which exhibits an exponential response, after applying a logarithmic transformation. Therefore, the two figures allow for a comparison of the direct linear response of the reference sensor with the linear form of the nonlinear response of the proposed sensor obtained after logarithmic transformation. During linearization, the mechanical behavior was modeled by Hooke's law ( $F = kx$ ); because the screen moves horizontally, light obstruction is proportional to spring compression ( $y = x$ ). The relationship between the amount of blocking of LED light ($y$) and the output voltage ($V_0$) can be expressed as follows, with the constants of the LED light (K) and the photo sensor (α).

$$V_o = Ke^{-\alpha y} \tag{1}$$

Combining $y = x$ with $F = kx \left( x = \frac{F}{k} \right)$ gives the system relation:

$$V_o = Ke^{\left(\frac{\alpha}{k}\right)F} \tag{2}$$

For linearization, a logarithmic transformation was applied, yielding:

$$ln\left(\frac{V_o}{V_{ref}}\right) = C + \left(\frac{\alpha}{k}\right)F, \qquad C = ln\left(\frac{K}{V_{ref}}\right) \tag{3}$$

Comparing the force–voltage graphs, the slope was calculated as 0.60 N/mV for the reference force sensor and 0.08 N/mV for the proposed optical sensing system. Under the experimental conditions used in this study, the optical sensor exhibited a more distinguishable response in the low-force region. In contrast, no stable and measurable output was observed from the RP-S40-ST sensor for loads below approximately 50 g within the present measurement setup. Therefore, the practical lower detection limit of the reference sensor was taken to be around this value under the applied calibration and signal acquisition conditions. This behavior is considered to be related not only to the intrinsic sensitivity of the sensor, but also to the characteristics of the experimental setup and the signal acquisition process.

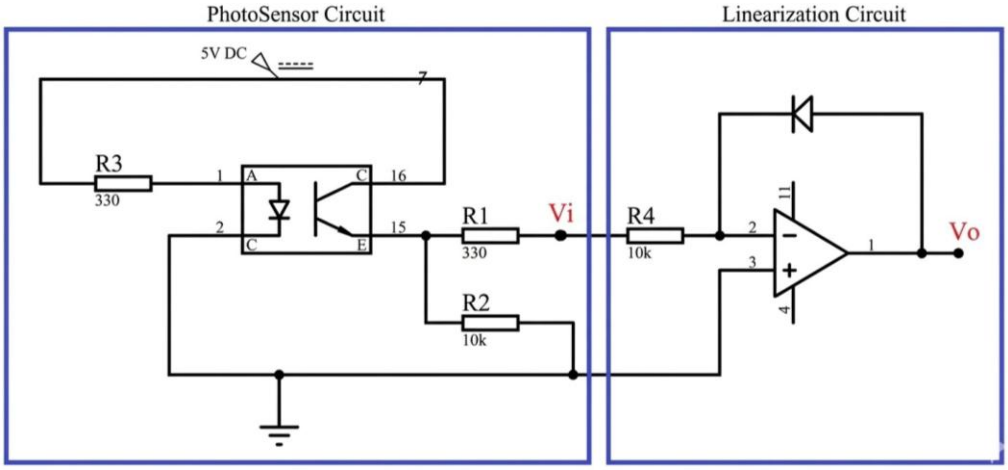



**Figure 5.** Linearization circuit

### 2.2.3.Circuit Design

In this study, the Arduino Mega is used as a microcontroller. Because Arduino Mega has limited analog input, we used a multiplexer (CD74HC4067). With this multiplexer, we were able to control 16 sensors in 1 analog input. In electronics, a multiplexer, also known as a data selector, is a device that selects between several analog

or digital input signals and forwards the selected input to a single output line. 4 sensor circuit diagrams with multiplexer and Arduino Mega shown in Figure 6.

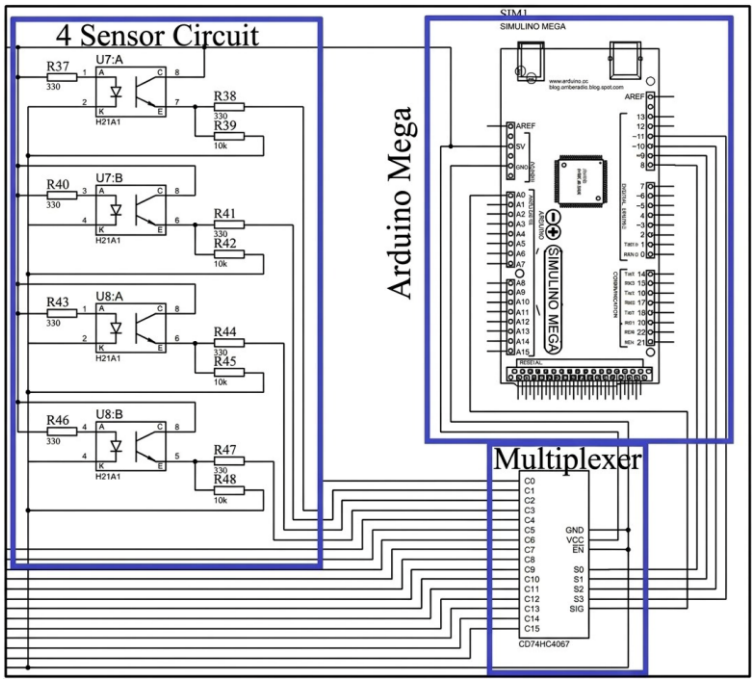



**Figure 6.** The schematic representation of a circuit for 4 sensors

The pseudocode in Figure 7 summarizes the basic operation of the multi-channel sensor reading mechanism designed based on Arduino. In the algorithm, each sensor channel is activated sequentially using a multiplexer selection table, and the analog output of the corresponding channel is read via the Arduino. After assigning the selection bits to the digital pins for each channel, a short waiting period is applied to support measurement stability. Then, the voltage value obtained from the analog input is scaled to be suitable for digital processing and saved to the sensor data vector. After repeating this process for all channels, the system collects the data from multiple sensors into a single output vector. Thus, the proposed structure allows for the regular, systematic, and scalable monitoring of many sensors with limited hardware resources.

**Algorithm 1** Multiplexer-Based Sensor Reading Procedure

**Require:** Arduino object $a$, multiplexer channel table $muxChannel$
**Ensure:** Sensor vector $x$
  $numChannels \leftarrow$ number of rows in $muxChannel$
  $x \leftarrow$ zero vector of length $numChannels$
3: **for** $channel = 1$ **to** $numChannels$ **do**
    $b_1 \leftarrow muxChannel(channel, 1)$, $b_2 \leftarrow muxChannel(channel, 2)$
    $b_3 \leftarrow muxChannel(channel, 3)$, $b_4 \leftarrow muxChannel(channel, 4)$
6: Write $b_1$ to digital pin D4
    Write $b_2$ to digital pin D5
    Write $b_3$ to digital pin D6
9: Write $b_4$ to digital pin D7
    Wait for 0.001 seconds
    Read voltage from analog pin A0
12: $x(channel) \leftarrow \dfrac{\text{Voltage} \times 1024}{5}$
  **end for**
  **return** $x$

**Figure 7.** Pseudocode for multiplexer-based sensor reading algorithm

### 2.3.Software Design

For object surface recognition, a MATLAB-based artificial neural network (ANN) approach was used for classification. The ANN model was developed and trained using MATLAB's neural network tools. During the initial data collection stage, three surface classes were selected for classification: flat-surfaced objects, serrated-surfaced objects, and wavy-surfaced objects. For these classes, 16 pattern samples with different combinations were designed and produced using a 3D printer.
The sensor values were transferred directly to the MATLAB environment, where the classification process was carried out using the ANN model. For pattern recognition, the sensor outputs corresponding to the surface pattern of each sample were used as feature vectors. After normalization, the acquired data were labeled according to the corresponding surface classes and then used in the classification stage.

The pseudocode in Figure 8 presents the general flow of the main control and classification algorithm. The algorithm first establishes the Arduino connection and defines the operating parameters of the system. It then continuously monitors the left movement, right movement, and sensor reading commands through the related digital input pins. When a left or right movement command is detected, the stepper motor is driven in the specified direction for the defined number of steps. When the sensor reading command is active, all sensor data are collected via the multiplexer, saved to a file, and transferred to the ANN model. Finally, the sensor values and classification output are displayed on the screen. This structure integrates motion control, data acquisition, and classification into a single real-time control framework.

**Algorithm 2** Arduino-Based Main Control and Classification

**Require:** Arduino object $a$, digital input pins D11, D12, D13, motor control pins D2 and D3, multiplexer selection table $muxChannel$
**Ensure:** Continuous motor control, sensor acquisition, and neural network classification

```
Connect to Arduino on COM8 using Mega2560
Wait for 3 seconds
stepsPerMove ← 20,   stepPulseDelay ← 0.002,   loopPause ← 0.2
while true do
    leftCmd ← read digital pin D12
    rightCmd ← read digital pin D13
    senseCmd ← read digital pin D11
    if leftCmd = 1 then
        Write direction value 1 to digital pin D2
        for k = 1 to stepsPerMove do
            Set digital pin D3 HIGH
            Wait for stepPulseDelay
            Set digital pin D3 LOW
            Wait for stepPulseDelay
        end for
        Wait for loopPause
    else if rightCmd = 1 then
        Write direction value 0 to digital pin D2
        for k = 1 to stepsPerMove do
            Set digital pin D3 HIGH
            Wait for stepPulseDelay
            Set digital pin D3 LOW
            Wait for stepPulseDelay
        end for
        Wait for loopPause
    else if senseCmd = 1 then
        x ← ReadAllSensors(a, muxChannel)
        Save x into matlab.mat
        result ← MyNeuralNetworkFunction(x, 1, 2)
        Display sensor values x
        Display neural network output result
        Wait for loopPause
    end if
end while
```

**Figure 8.** Pseudocode for main control and classification algorithm

The classification model was implemented in MATLAB using the Neural Net Pattern Recognition framework as a shallow feedforward artificial neural network. The network consisted of 16 input neurons corresponding to the voltage values obtained from the 4×4 tactile sensor array, a single hidden layer with 20 neurons, and an output layer with a number of neurons equal to the number of target classes. The output layer used a SoftMax activation function for multi-class classification. The model was trained using the MATLAB pattern recognition environment, and the remaining training settings followed the default MATLAB configuration.

## 3.Classification and Training

Artificial Neural Network (ANN), which imitates the functioning of the human nervous system, tries to reveal the hidden relationships in the data structure by using the data related to the problem at hand. This operation of the network is called learning. The data coming from the sensor is transferred to the MATLAB environment after being subjected to the necessary processes by Arduino. The sensor presents a voltage value as output over the Arduino. This value ranges from 0 to 5V. The value changes depending on the shape change of the object placed on the system. For example, when a heavy object is placed on the system, the obtained value approaches 0, while this value becomes higher depending on the surface shape of the object. These values are displayed instantly by Arduino on the output screen.

In this study, the classification stage was based on the outputs collected from the 4×4 tactile sensor array. Each measurement sample consisted of the voltage values obtained from the 16 sensors after contact between the gripper and the test surface. Therefore, each sample was represented as a 16-dimensional input vector and used as the input of the ANN model. These input vectors reflected the spatial response of the sensor array to the contacted surface and represented the surface pattern of the object.

After the acquisition stage, the sensor values were transferred directly to the MATLAB environment, where the pattern recognition process was carried out using the ANN model. Before classification, the acquired sensor values were normalized to provide a consistent input range for the ANN. After normalization, each input vector was assigned a class label according to the corresponding surface pattern and then used in the supervised classification stage. At this stage, pieces with different patterns were deliberately chosen to avoid memorization. Instead of using many parts with the same characteristics, this possibility was minimized by using parts with different characteristics, as shown in Figure 9.

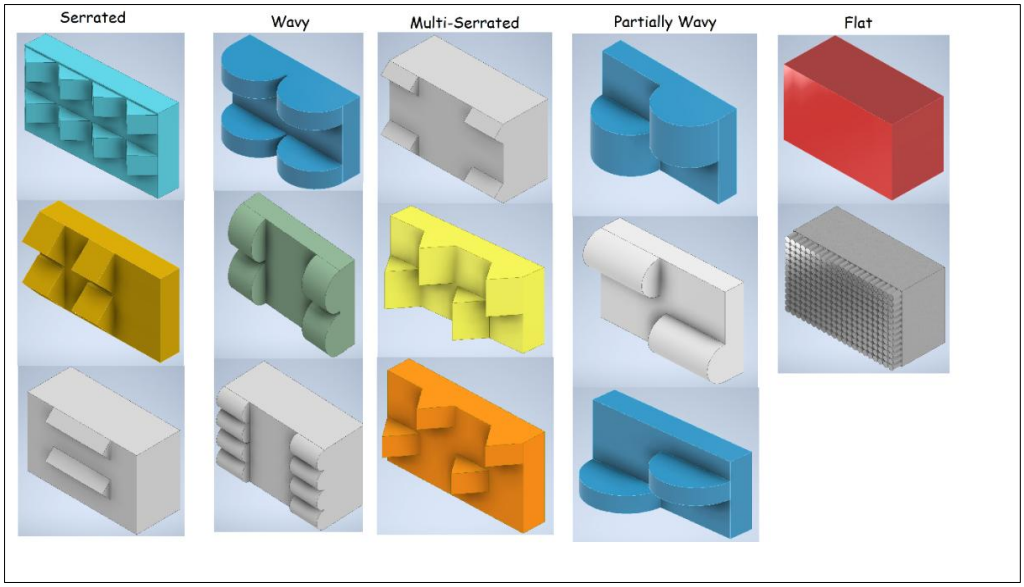



**Figure 9.** Patterns with different surface characteristics

To increase the number of available data points and to use the sensor array in the most efficient way possible, parts with different surface patterns were shifted on the sensor array, and data was collected from each sensor according to different positions shown in Figure 10. In this way, multiple input vectors were obtained for the

same surface type under different contact locations, which increased dataset diversity and reduced the possibility of memorization. A total of 2500 data points were collected. To follow a more standard supervised learning protocol, the dataset was divided into training, validation, and test subsets, with 70% of the samples used for training, 15% for validation, and 15% for testing.

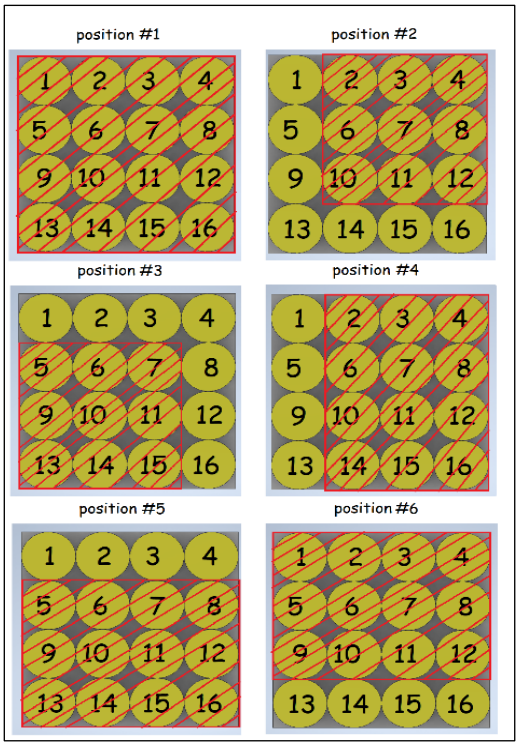



**Figure 10.** Pattern shifting positions

In classification tasks, the term target class refers to the category or label assigned to each data point. In this study, the target classes correspond to the defined surface patterns shown in Figures 10 and 11. To evaluate the performance of the classification model, confusion matrices were used for both the experimental and theoretical cases. In these matrices, each row represents the actual class and each column represents the predicted class. The diagonal elements indicate correct classifications, whereas the off-diagonal elements represent misclassifications. The overall classification accuracy is calculated as the ratio of correctly classified samples to the total number of samples.

The confusion matrix obtained under experimental conditions is presented in Figure 11. The experimental analysis was performed using a more detailed class structure, in which additional surface variations were included in the dataset. As a result, the experimental confusion matrix contains a larger number of classes and reflects the performance of the model under more realistic and diverse testing conditions.

The analysis of the experimental confusion matrix shown in Figure 11 reveals consistent performance across all datasets. The training set achieved the highest accuracy, with 94.2% of instances correctly classified. The validation and test sets both yielded an accuracy of 93.3%, demonstrating that the model generalized well to unseen data. Since there was no significant performance decrease from the training set to the validation and test sets, the model did not show noticeable overfitting. When all datasets were considered together, the model achieved an overall accuracy of 94.0%, indicating stable and reliable classification performance.

For comparison, the idealized class prediction structure is illustrated in Figure 12. Unlike the experimental case, the theoretical confusion matrix was constructed using a simplified class definition based on the main surface categories. Therefore, it contains fewer classes and serves as a conceptual reference for ideal classification behavior. In this matrix, all correctly classified samples are located on the diagonal, while the off-diagonal

elements are zero. This representation provides a reference for evaluating the deviation of the experimental results from the ideal classification case.

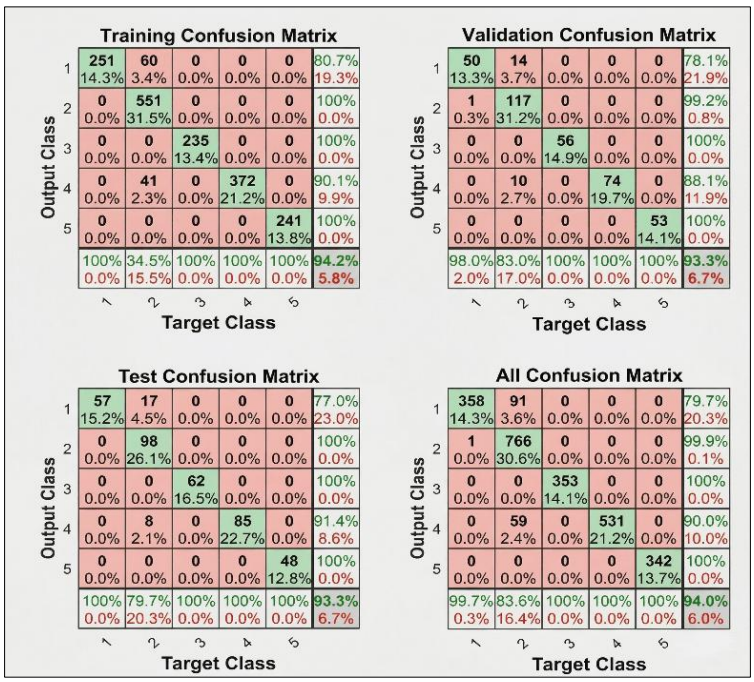



**Figure 11.** Confusion matrix in experimental setting

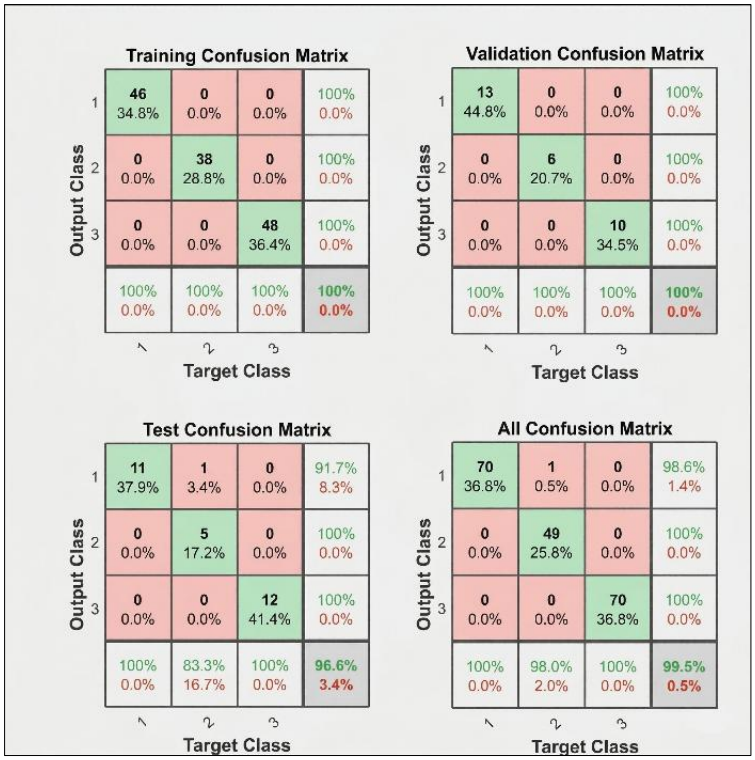



**Figure 12.** Confusion matrix in a theoretical setting

## 4.Conclusions

In this study, we presented a new cost-effective tactile sensing system that utilizes optical technology. Equipped with a sensor array for surface shape detection, this system can measure different force values when pressure is

applied by external objects. The system's unique ability to convert applied force into an optical signal has been instrumental in perceiving the shapes of various surfaces. Force detection sensors in the system enable the robotic gripping mechanism to determine mechanical deformation according to the detected signal and classify surfaces according to their texture. The system has proven effective in classifying structures through the recognition process, thanks to a 4×4 sensor array containing only 16 sensors and the application of machine learning techniques. Objects within the system exhibit irregular patterns that form a variety of structural shapes, resulting in fluctuations in perceived optical density based on surface patterns such as wavy, flat, or edged, which are affected by the applied force. The system achieved a 94.2% success rate in determining surface profiles, highlighting its reliability and accuracy.

In practical terms, the proposed system has potential applications in industrial part sorting, robotic grasp feedback, and surface-based quality control. Since the developed tactile array can distinguish different surface patterns through ANN-based classification, it may be used in production environments where contact-based identification of flat, wavy, serrated, or similarly structured surfaces is required. Its compact and low-cost structure also makes it suitable for integration into robotic grippers and simple automation systems where surface recognition and object classification are needed.

As a result, the designed system shows strong potential for applications requiring the recognition and separation of mechanical parts, particularly in industrial and robotic environments. The success of this study paves the way for further research and development in this field, potentially leading to more advanced and efficient tactile sensing systems in the future.

## Declaration of Competing Interest

No conflict of interest was declared by the authors.

## Authorship Contribution Statement

**Yusuf Buğra Günaydın:** Conceptualization, Methodology, Software, Investigation, Writing – original draft
**Elif Safel:** Formal analysis, Investigation, Validation, Visualization
**Ahmet Gökay Çalış:** Visualization, Writing – review and editing
**Çağlar Arpali:** Supervision

## References

[1] Z. Kappassov, J.-A. Corrales, and V. Perdereau, “Tactile sensing in dexterous robot hands—Review,” Robot. Auton. Syst., vol. 74, pp. 195–220, Dec. 2015, doi: 10.1016/j.robot.2015.07.015.
[2] Y. Al-Handarish et al., “A survey of tactile-sensing systems and their applications in biomedical engineering,” Adv. Mater. Sci. Eng., vol. 2020, Art. no. 4047937, Jan. 2020, doi: 10.1155/2020/4047937.
[3] C. Chi, X. Sun, N. Xue, T. Li, and C. Liu, “Recent progress in technologies for tactile sensors,” Sensors, vol. 18, no. 4, Art. no. 948, Apr. 2018, doi: 10.3390/s18040948.
[4] C. W. de Silva, Sensors and Actuators: Engineering System Instrumentation, 2nd ed. Boca Raton, FL, USA: CRC Press, 2015.
[5] S. Zhang, Z. Chen, Y. Gao, W. Wan, and H. A. Varol, “Hardware technology of vision-based tactile sensor: A review,” IEEE Sens. J., vol. 22, no. 22, pp. 21410–21427, Nov. 2022, doi: 10.1109/JSEN.2022.3210210.
[6] Q. Sun, B. He, C. Xiong, W. Zhang, and H. A. Varol, “Force measurement technology of vision-based tactile sensor,” Adv. Intell. Syst., Jan. 2025, doi: 10.1002/aisy.202400290.
[7] W. Yuan, S. Dong, and E. H. Adelson, “GelSight: High-resolution robot tactile sensors for estimating geometry and force,” Sensors, vol. 17, no. 12, Art. no. 2762, Dec. 2017, doi: 10.3390/s17122762.
[8] B. Ward-Cherrier et al., “The TacTip family: Soft optical tactile sensors with 3D-printed biomimetic morphologies,” Soft Robot., vol. 5, no. 2, pp. 216–227, Apr. 2018, doi: 10.1089/soro.2017.0052.
[9] M. Lambeta et al., “DIGIT: A novel design for a low-cost compact high-resolution tactile sensor with application to in-hand manipulation,” IEEE Robot. Autom. Lett., vol. 5, no. 3, pp. 3838–3845, Jul. 2020, doi: 10.1109/LRA.2020.2977257.
[10] N. Funk et al., “Evetac: An event-based optical tactile sensor for robotic manipulation,” IEEE Trans. Robot., vol. 40, 2024, doi: 10.1109/TRO.2024.3428430.
[11] K. Sato, K. Kamiyama, N. Kawakami, and S. Tachi, “Finger-shaped GelForce: Sensor for measuring surface traction

fields for robotic hand," IEEE Trans. Haptics, vol. 3, no. 1, pp. 37–47, Jan. 2010, doi: 10.1109/TOH.2009.47.
[12] H. Xie, A. Jiang, L. Seneviratne, and K. Althoefer, "Pixel-based optical fiber tactile force sensor for robot manipulation," in Proc. IEEE Sensors, Oct. 2012, doi: 10.1109/ICSENS.2012.6411462.
[13] P. Kampmann and F. Kirchner, "A tactile sensing system for underwater manipulation," in Proc. Workshop on Advances in Tactile Sensing and Touch-Based Human-Robot Interaction (HRI), Boston, MA, USA, Mar. 2012.
[14] L. Massari et al., "Tactile sensing and control of robotic manipulator integrating fiber Bragg grating strain-sensor," Front. Neurorobot., vol. 13, Art. no. 8, Feb. 2019, doi: 10.3389/fnbot.2019.00008.
[15] Z. Kappassov et al., "Color-coded fiber-optic tactile sensor for an elastomeric robot skin," in Proc. IEEE Int. Conf. Robot. Autom. (ICRA), May 2019, doi: 10.1109/ICRA.2019.8793262.
[16] J. B. Jeong, H. Kim, and J.-I. Yoo, "Triboelectric touch sensor for position mapping during total hip arthroplasty," BMC Res. Notes, vol. 13, no. 1, Art. no. 395, Aug. 2020, doi: 10.1186/s13104-020-05238-4.